

Published in final edited form as:

*Clin Biomech (Bristol, Avon)*. 2013 January ; 28(1): 10–14. doi:10.1016/j.clinbiomech.2012.10.005.

## Longitudinal Changes in Lumbar Bone Mineral Density Distribution May Increase the Risk of Wedge Fractures

Hugo Giambini, B.S.<sup>1</sup>, Sundeep Khosla, M.D.<sup>2</sup>, Ahmad Nassr, M.D.<sup>1,3</sup>, Chunfeng Zhao, M.D.<sup>1</sup>, and Kai-Nan An, Ph.D.<sup>1</sup>

<sup>1</sup>Biomechanics Laboratory, Division of Orthopedic Research, Mayo Clinic, Rochester, Minnesota USA

<sup>2</sup>Division of Endocrinology, Metabolism and Nutrition, Department of Internal Medicine, College of Medicine Mayo Clinic, Rochester, Minnesota USA

<sup>3</sup>Department of Orthopedic Surgery, Mayo Clinic, Rochester, Minnesota USA

### Abstract

**Background**—Trabecular bone strength diminishes as a result of osteoporosis and altered biomechanical loading at the vertebral and spine level. The spine consists of the anterior, middle and posterior columns and the load supported by the anterior and middle columns will differ across different regions of the spine. Stress shielding of the anterior column can contribute to bone loss and increase the risk of wedge fracture. There is a lack of quantitative data related to regional spinal bone mineral density distribution over time. We hypothesize that there is an increase in the posterior-to-anterior vertebral body bone mineral density ratio and a decrease in whole-body bone mineral density over time.

**Methods**—Bone mineral density was measured in 33 subjects using quantitative computed tomography scans for L1–L3 vertebrae, region (anterior and posterior vertebral body), and time (baseline and 6 years after).

**Findings**—Lumbar bone mineral density decreased significantly ( $\Delta$ : ~15%) from baseline to the 6<sup>th</sup> year visit. Individual vertebrae differences over time (L1: ~14%, L2: ~14%, L3: ~17%) showed statistical significance. Anterior bone mineral density change was significantly greater than in the posterior vertebral body region ( $\Delta$  anterior: ~18%;  $\Delta$  posterior: ~13%). Posterior-to-anterior bone mineral density ratio was significantly greater in the 6<sup>th</sup> year compared to baseline values (mean (SD), 1.33 (0.2) vs. 1.23 (0.1)).

**Interpretation**—This study provides longitudinal quantitative measurement of bone mineral density in vertebrae as well as regional changes in the anterior and posterior regions. Understanding bone mineral density distribution over time may help to decrease the risk of wedge fractures if interventions can be developed to bring spine loading to its normal state.

### Keywords

Lumbar; Bone Mineral Density; Time; Risk of Fracture; Vertebrae

© 2012 Elsevier Ltd. All rights reserved.

Corresponding Author: Kai-Nan An, Ph.D., Mayo Clinic, 200 First Street SW, Rochester, MN 55905, Phone: 507-538-1717, Fax: 507-284-5392, an.kainan@mayo.edu.

**Publisher's Disclaimer:** This is a PDF file of an unedited manuscript that has been accepted for publication. As a service to our customers we are providing this early version of the manuscript. The manuscript will undergo copyediting, typesetting, and review of the resulting proof before it is published in its final citable form. Please note that during the production process errors may be discovered which could affect the content, and all legal disclaimers that apply to the journal pertain.

## Introduction

Osteoporosis is characterized by low bone mass, decreased bone strength, architectural deterioration and a significant increase in fracture risk and bone fragility (Briggs et al., 2006; Homminga et al., 2004; Imai et al., 2009; Kayanja et al., 2004) (Wang H-J et al., 2012). Osteoporosis is a silent and asymptomatic disease usually not diagnosed until a person presents with an insufficiency fracture or after fractures have already occurred, thus delaying necessary treatment (Kayanja et al., 2004; McDonnell et al., 2007; Melton and Kallmes, 2006). Vertebral fractures often occur as a result of normal daily loads and may be clinically undetected (Homminga et al., 2004; Homminga et al., 2001; Imai et al., 2006; Kayanja et al., 2004). However these fractures can be associated with significant functional limitations. (Nevitt et al., 1998)

Fracture risk is affected by loading changes at the regional and local levels. At the local vertebral level, it has been reported (Rockoff et al., 1969) that the cortical shell contributes about 45–75% of the vertebral strength, however Homminga et al. demonstrated that trabecular bone carries 50–70% of the total load. (Homminga et al., 2004; Homminga et al., 2001). At the regional level, many factors affect spine loading including the sagittal alignment of the thoracic and lumbar spine. (Kobayashi et al., 2008). Denis et al. described the spine as three columns (Denis, 1983): “anterior (anterior half of the vertebral body), middle (posterior half of vertebral body), and posterior (pedicles, posterior elements and facets) columns”. The majority of the load is transmitted through the anterior and middle columns but differs across regions of the spine. Degenerative changes with time result in decreased load in the anterior column, and increased across the middle and posterior columns (Adams and Hutton, 1983) (Pollintine et al., 2004). This shielding of the anterior column may contribute to bone loss and an increase in wedge fracture risk over time (Pollintine et al., 2004).

This posterior shift in loading that occurs with aging is not picked up by traditional bone mineral density (BMD) testing. Little has been published in current literature regarding these local changes in the vertebral BMD over time. Specifically does posterior vertebral BMD increase relative to anterior BMD over time? We hypothesize that with aging, there will be a total decrease in vertebral body BMD, but an increase in the posterior-to-anterior vertebral body BMD ratio over time. In order to investigate these changes we performed a longitudinal analysis of BMD changes in the L1–L3 vertebrae on a cohort of patients followed for a period of six years.

## Methods

### Study Subjects

We utilized data previously collected as part of an ongoing study that has previously been described (Riggs et al., 2004). Twenty-one males with no history of fracture or bone spurs/endplate deformations and 12 males with at least one grade 2–3 thoracic vertebral fracture were included. Severe thoracic vertebral fractures (grade 2–3) were classified as a reduction of approximately 25% or greater in anterior/middle and/or posterior height, as previously described (Genant and Jergas, 2003; Melton et al., 2010). Subjects were selected so that they had approximately the same age and BMI (body mass index) (Table 1). All subjects had quantitative computed tomography (QCT) scans of the lumbar spine (L1, L2 and L3) obtained as part of the original study after they had provided written informed consent.

## Bone Density Measurements

As previously described (Melton et al., 2010), QCT images of the lumbar region (L1, L2 and L3) were obtained by single-energy QCT using two different scanners over the course of the original study. Briefly, a 4-channel multidetector-row scanner (LightSpeed Qx/i) and a 64-channel system (Somatom Sensation 64) from Siemens Healthcare (Forchheim, Germany), with the same scanning parameters, were used for the image acquisition at both time points (Baseline and 6<sup>th</sup> years after). The baseline external calibration standard, Model 2 Liquid Phantom, was changed at the 6<sup>th</sup> year to a Model 3 Solid Phantom (Mindways Software, Inc., Austin, TX, USA).

The QCT-DICOM images were analyzed with Mimics image processing and editing software (Materialise US, Ann Arbor, MI USA). Segmentation was performed in vertebral body trabecular bone regions of L1, L2 and L3 at two time points, baseline and 6-years after. A standard Hounsfield unit (HU) window ( $HU > 225$ ) was applied to define the cortical bone in each scan for all vertebrae (Figure 1A). Region growing operations allowed the vertebral body cortical bone to be separated from pixels inside and outside the vertebral cortical region that had similar HU intensity values but were not part of the cortex. The posterior vertebral body boundary was defined by a line passing through the middle of the neural arch and aligned with the coronal plane. Using image editing, regions of the cortex that were not included in the mask were incorporated to make a closed perimeter around the vertebral body (Figure 1B). Polylines were subsequently created around the cortex and the enclosed region, including cortical and trabecular bone, segmented (Figure 1C). By performing subtractive Boolean operations of the cortical and newly formed mask, whole body trabecular bone, excluding the cortex, was then segmented in all vertebrae (Figure 1D). This new mask contained the entire vertebral body without cortical bone.

For all vertebrae (L1–L3), anterior and posterior vertebral body regions were created from the original whole-body segmentations based on the spine sagittal view and inertia axis. A coronal slice mid-way between the superior and inferior endplates and a slice passing through approximately the middle of the vertebrae in the sagittal plane were selected. To obtain the inertia axis, a 3D object of the already segmented slice in the coronal plane was created (Figure 1E). Also, a line was drawn in the sagittal plane slice joining the superior dorsal and inferior dorsal points of the vertebral cortex (Figure 1F). A plane in the direction of the line and passing through the inertia axis in the coronal plane was drawn to divide the anterior and posterior vertebral regions (Figure 1G). Again, by performing subtractive Boolean operations and region growing with the whole-body mask, the anterior and posterior vertebral body trabecular regions were obtained. Region growing operations allowed for individual masks containing the L1, L2 and L3 whole body, anterior and posterior trabecular regions (Figure 1H and 1I). Trabecular Hounsfield units from all three segmentations (whole vertebral body, anterior and posterior region) for all vertebrae were exported in text-based format. Calibration phantoms (Models 2 and 3) containing reference material were used to obtain equivalent  $K_2HPO_4$  densities of the unknown vertebrae regions using a custom linear regression program in MATLAB (Mathworks, Natick, MA). Equivalent  $K_2HPO_4$  densities were obtained for each site (L1, L2 and L3), region (anterior and posterior), and time (baseline and 6 years after) for all 33 subjects.

## Statistical Analysis

Data analyses were completed using SAS (SAS Institute Inc., Cary, NC USA). A repeated measures analysis of variance model was run to test for overall differences between vertebrae sites (L1, L2, and L3), regions (posterior and anterior) and time (baseline and 6 years after); interactions between the different factors were also analyzed.

## Results

There were no statistically significant differences in age or BMI between the 21 controls and the 12 males with grade 2–3 non-lumbar fractures (Table 1). Furthermore, there were no statistically significant differences in any of the measured values (whole body, anterior and posterior body BMD's, either at baseline or 6<sup>th</sup> year). For this reason, the subjects were combined into one pool of data comprising of 33 male subjects. Data presented corresponds to the pooled data. Figure 2 describes the measured BMD per site and region for the 33 subjects. Lumbar (L1–L3) BMD decreased significantly ( $\Delta$ : ~15%) from 140.3 (37.9) mg/cm<sup>3</sup> at baseline to 119 (38.8) mg/cm<sup>3</sup> at the 6<sup>th</sup> year visit ( $P<0.0001$ ) (Figure 3). There was also a statistical difference ( $P=0.0136$ ) between sites over time, with BMD decreasing ~14% in L1, ~14% in L2 and 17% in L3 (Figure 4). Lumbar anterior vertebral body BMD decrease over time was significantly greater ( $P=0.0177$ ) than in the posterior body region (anterior-baseline: 126 (32.9), anterior-6<sup>th</sup> year: 103.8 (33.9),  $\Delta$  anterior: ~18%; posterior-baseline: 154 (37.7), posterior-6<sup>th</sup> year: 134.2 (37.5) mg/cm<sup>3</sup>,  $\Delta$  posterior: ~13%) (Figure 5). Posterior-to-anterior BMD ratio was significantly greater in the 6<sup>th</sup> year compared to baseline values (mean (SD), 1.33 (0.2) vs. 1.23 (0.1),  $P<0.0001$ ) (Figure 6).

## Discussion

In this study we were able to quantify the BMD of the lumbar region (L1–L3) in 33 male subjects based on QCT images at two different time points. We found the lumbar trabecular BMD to significantly decrease in a six year span and these differences varied significantly between vertebrae, with L3 having the highest change in BMD. The anterior vertebral region demonstrated a significant decrease compared to the posterior vertebral region. This resulted in a significant difference in the posterior-to-anterior ratio over time.

This study was motivated by the lack of quantitative data in the literature relating local lumbar trabecular changes in BMD over time. While many studies support a posterior shift in loading we are not aware of any studies that show that this translates into BMD changes in the posterior vertebral body. The results support our hypothesis that BMD decreases with time and that there is an increase in posterior-to-anterior BMD ratio in the lumbar region. These data also support previous literature reports stating stress shielding of the anterior column as a cause and contributor of bone loss (Pollintine et al., 2004).

Disc degeneration (Pollintine et al., 2004), age (Andresen et al., 1998) (Melton et al., 2006) and changes in the sagittal alignment of the spine (Kobayashi et al., 2008) have been associated with decreases in vertebral loading. With age, vertebral load is shifted to the facet joints thereby decreasing anterior BMD and the strength of the vertebral body, possibly increasing wedge fracture risk (Pollintine et al., 2004). Disc degeneration causes a shift in vertebral load and is associated to changes in trabecular and cortical BMD (Homminga et al., 2012; Wang et al., 2011). Spine curvature changes, including scoliosis, kyphotic and lordotic changes can also contribute to abnormal loading on the vertebrae, which may increase the risk of fracture (Watanabe et al., 2007) (Li et al., 2008). These changes in spinal alignment have been linked with the development of osteoporosis (Sadat-Ali et al., 2008) (Routh et al., 2005) (Watanabe et al., 2007). Other studies have demonstrated that thoracic kyphosis is significantly and inversely correlated with lumbar BMD (Edmondston et al., 1994) (Ettinger et al., 1994; Thevenon et al., 1987; Kobayashi, 2008 #18).

At the local vertebrae level, previous studies have shown the contribution of the cortical shell and trabecular bone in the load bearing capacity and fracture risk of the vertebra (Andresen et al., 1998; Cao et al., 2001; Cody et al., 1991; Eswaran et al., 2006; Homminga et al., 2004; Homminga et al., 2001). However, these studies have not demonstrated BMD

changes and distribution within and between vertebral bodies and their association with fracture risk.

A relative decrease in anterior-to-posterior BMD may predispose to wedge fractures in patients with osteoporosis. As previously described, flattening of the lumbar spine results in a forward shift and sagittal imbalance, multiple disc degeneration, and a higher load in the anterior portion of the vertebral body (Gelb DE et al., 1995; Hammerberg EM and KB., 2003; Kobayashi et al., 2008). Understanding longitudinal curvature changes and BMD distribution within the vertebral body is of significant importance in preventive medicine. Specific interventions targeting this differential bone loss in the anterior body may decrease the risk of wedge fractures through bracing, therapy and other modalities aimed at normalizing spine loading. A better understanding of individual vertebrae, other than the lumbar (L1–L3) analyzed in this study will also contribute greatly to our understanding of these changes over time. Other factors associated with the development of osteoporotic vertebral fractures need to continue to be studied including: the role of muscle activity, micro-architecture and intrinsic material properties of bone.

This study has several limitations. First, the small subject number may have affected our results; however based on our observations, we believe that these findings would be similar in a larger study. Second, even though calibration phantoms were used for both (baseline and 6<sup>th</sup> year) scanning times, there might have been some variability in the image acquisition affecting the density measurements. Third, only the lumbar (L1–L3) region was acquired in the QCT scan, preventing us from drawing any conclusions at other spinal regions. Also, we were unable to measure spine curvature in the study population, preventing us from reaching conclusions between BMD distribution and spinal alignment. In addition to the small population number, spinal alignment and/or the degree of disc degeneration between the controls and the fractured population might have been an additional cause for not finding differences between the groups. Lastly, we were unable to measure the degree of disc degeneration thus preventing us from reaching concluding remarks between the longitudinal causes of BMD loss and the degenerative process.

## Conclusions

In summary, BMD changes in the anterior, posterior and whole vertebral bodies (L1–L3) of 33 human subjects were quantified and measured from QCT images at two different time points. BMD in the lumbar region was shown to decrease and the posterior-to-anterior ratio to increase over time. These findings support previous hypotheses of a posterior load shift in the spine over time and lead to a better understanding between BMD changes and individual vertebral body measurements. This posterior shift in load bearing seen with aging and degenerative change in the spine may result in stress shielding of the anterior vertebral body that ultimately contributes the development of osteoporotic wedge fractures.

## Acknowledgments

The authors would like to thank Sara J. Achenbach and Elizabeth Atkinson, from the Division of Biostatistics at Mayo Clinic, for their assistance in the statistical analysis.

This project was supported by internal funding from the Mayo foundation and Grant numbers R01 AR027065 (SK) and UL1TR000135 (Mayo CTSA) from the National Institutes of Health (NIH). The study sponsors had no role in the study design, collection, analysis or interpretation of data.

## References

1. Adams MA, Hutton WC. The mechanical function of the lumbar apophyseal joints. *Spine*. 1983; 8:327–330. [PubMed: 6623200]

2. Andresen R, Werner HJ, Schober HC. Contribution of the cortical shell of vertebrae to mechanical behaviour of the lumbar vertebrae with implications for predicting fracture risk. *Br J Radiol.* 1998; 71:759–765. [PubMed: 9771387]
3. Briggs AM, Wrigley TV, van Dieen JH, Phillips B, Lo SK, Greig AM, et al. The effect of osteoporotic vertebral fracture on predicted spinal loads in vivo. *Eur Spine J.* 2006; 15:1785–1795. [PubMed: 16819622]
4. Cao KD, Grimm MJ, Yang KH. Load sharing within a human lumbar vertebral body using the finite element method. *Spine.* 2001; 26:E253–260. [PubMed: 11426165]
5. Cody DD, Goldstein SA, Flynn MJ, Brown EB. Correlations between vertebral regional bone mineral density (rBMD) and whole bone fracture load. *Spine.* 1991; 16:146–154. [PubMed: 2011769]
6. Denis F. The three column spine and its significance in the classification of acute thoracolumbar spinal injuries. *Spine.* 1983; 8:817–831. [PubMed: 6670016]
7. Edmondston SJ, Singer KP, Price RI, Day RE, Breidahl PD. The relationship between bone mineral density, vertebral body shape and spinal curvature in the elderly thoracolumbar spine: an in vitro study. *Br J Radiol.* 1994; 67:969–975. [PubMed: 8000841]
8. Eswaran SK, Gupta A, Adams MF, Keaveny TM. Cortical and trabecular load sharing in the human vertebral body. *J Bone Miner Res.* 2006; 21:307–314. [PubMed: 16418787]
9. Ettinger B, Black DM, Palermo L, Nevitt MC, Melnikoff S, Cummings SR. Kyphosis in older women and its relation to back pain, disability and osteopenia: the study of osteoporotic fractures. *Osteoporos Int.* 1994; 4:55–60. [PubMed: 8148573]
10. Gelb DE, Lenke LG, Bridwell KH, Blanke K, KWM. An analysis of sagittal spinal alignment in 100 asymptomatic middle and older aged volunteers. *Spine.* 1995; 20:1351–1358. [PubMed: 7676332]
11. Genant HK, Jergas M. Assessment of prevalent and incident vertebral fractures in osteoporosis research. *Osteoporos Int.* 2003; 14(Suppl 3):S43–55. [PubMed: 12730798]
12. Hammerberg EM, KBW. Sagittal profile of the elderly. *J Spinal Disord Tech.* 2003; 16:44–50. [PubMed: 12571484]
13. Homminga J, Aquarius R, Bultink VE, Jansen CT, Verdonchot N. Can vertebral density changes be explained by intervertebral disc degeneration? *Med Eng Phys.* 2012; 34:453–458. [PubMed: 21893424]
14. Homminga J, Van-Rietbergen B, Lochmuller EM, Weinans H, Eckstein F, Huiskes R. The osteoporotic vertebral structure is well adapted to the loads of daily life, but not to infrequent “error” loads. *Bone.* 2004; 34:510–516. [PubMed: 15003798]
15. Homminga J, Weinans H, Gowin W, Felsenberg D, Huiskes R. Osteoporosis changes the amount of vertebral trabecular bone at risk of fracture but not the vertebral load distribution. *Spine.* 2001; 26:1555–1561. [PubMed: 11462085]
16. Imai K, Ohnishi I, Bessho M, Nakamura K. Nonlinear finite element model predicts vertebral bone strength and fracture site. *Spine.* 2006; 31:1789–1794. [PubMed: 16845352]
17. Imai K, Ohnishi I, Matsumoto T, Yamamoto S, Nakamura K. Assessment of vertebral fracture risk and therapeutic effects of alendronate in postmenopausal women using a quantitative computed tomography-based nonlinear finite element method. *Osteoporos Int.* 2009; 20:801–810. [PubMed: 18800178]
18. Kayanja MM, Ferrara LA, Lieberman IH. Distribution of anterior cortical shear strain after a thoracic wedge compression fracture. *Spine J.* 2004; 4:76–87. [PubMed: 14749196]
19. Kobayashi T, Takeda N, Atsuta Y, Matsuno T. Flattening of sagittal spinal curvature as a predictor of vertebral fracture. *Osteoporos Int.* 2008; 19:65–69. [PubMed: 17874033]
20. Li XF, Li H, Liu ZD, Dai LY. Low bone mineral status in adolescent idiopathic scoliosis. *Eur Spine J.* 2008; 17:1431–1440. [PubMed: 18751741]
21. McDonnell P, McHugh PE, O’Mahoney D. Vertebral osteoporosis and trabecular bone quality. *Ann Biomed Eng.* 2007; 35:170–189. [PubMed: 17171508]
22. Melton LJ 3rd, Kallmes DF. Epidemiology of vertebral fractures: implications for vertebral augmentation. *Acad Radiol.* 2006; 13:538–545. [PubMed: 16627192]

23. Melton LJ 3rd, Riggs BL, Achenbach SJ, Amin S, Camp JJ, Rouleau PA, et al. Does reduced skeletal loading account for age-related bone loss? *J Bone Miner Res.* 2006; 21:1847–1855. [PubMed: 17002566]
24. Melton LJ 3rd, Riggs BL, Keaveny TM, Achenbach SJ, Kopperdahl D, Camp JJ, et al. Relation of vertebral deformities to bone density, structure, and strength. *J Bone Miner Res.* 2010; 25:1922–1930. [PubMed: 20533526]
25. Nevitt MC, Ettinger B, Black DM, Stone K, Jamal SA, Ensrud K, et al. The association of radiographically detected vertebral fractures with back pain and function: a prospective study. *Ann Int Med.* 1998; 128:793–800. [PubMed: 9599190]
26. Pollintine P, Dolan P, Tobias JH, Adams MA. Intervertebral disc degeneration can lead to “stress-shielding” of the anterior vertebral body: a cause of osteoporotic vertebral fracture? *Spine.* 2004; 29:774–782. [PubMed: 15087801]
27. Riggs BL, Melton LJ 3rd, Robb RA, Camp JJ, Atkinson EJ, Peterson JM, et al. Population-based study of age and sex differences in bone volumetric density, size, geometry, and structure at different skeletal sites. *J Bone Miner Res.* 2004; 19:1945–1954. [PubMed: 15537436]
28. Rockoff SD, Sweet E, Bleustein J. The relative contribution of trabecular and cortical bone to the strength of human lumbar vertebrae. *Calcif Tissue Res.* 1969; 3:163–175. [PubMed: 5769902]
29. Routh RH, Rumancik S, Pathak RD, Burshell AL, Nauman EA. The relationship between bone mineral density and biomechanics in patients with osteoporosis and scoliosis. *Osteoporos Int.* 2005; 16:1857–1863. [PubMed: 15999291]
30. Sadat-Ali M, Al-Othman A, Bubshait D, Al-Dakheel D. Does scoliosis causes low bone mass? A comparative study between siblings. *Eur Spine J.* 2008; 17:944–947. [PubMed: 18427842]
31. Thevenon A, Pollez B, Cantegrit F, Tison-Muchery F, Marchandise X, Duquesnoy B. Relationship between kyphosis, scoliosis, and osteoporosis in the elderly population. *Spine.* 1987; 12:744–745. [PubMed: 3686229]
32. Wang H-J, Giambini H, Zhang W-J, Ye G-H, Zhao C, et al. A Modified Sagittal Spine Postural Classification and Its Relationship to Deformities and Spinal Mobility in a Chinese Osteoporotic Population. *PLoS ONE.* 2012; 7:e38560. doi:38510.31371/journal.pone.0038560. [PubMed: 22693647]
33. Wang YX, Griffith JF, Ma HT, Kwok AW, Leung JC, Yeung DK, et al. Relationship between gender, bone mineral density, and disc degeneration in the lumbar spine: a study in elderly subjects using an eight-level MRI-based disc degeneration grading system. *Osteoporos Int.* 2011; 22:91–96. [PubMed: 20352410]
34. Watanabe G, Kawaguchi S, Matsuyama T, Yamashita T. Correlation of scoliotic curvature with Z-score bone mineral density and body mass index in patients with osteogenesis imperfecta. *Spine.* 2007; 32:E488–494. [PubMed: 17762282]

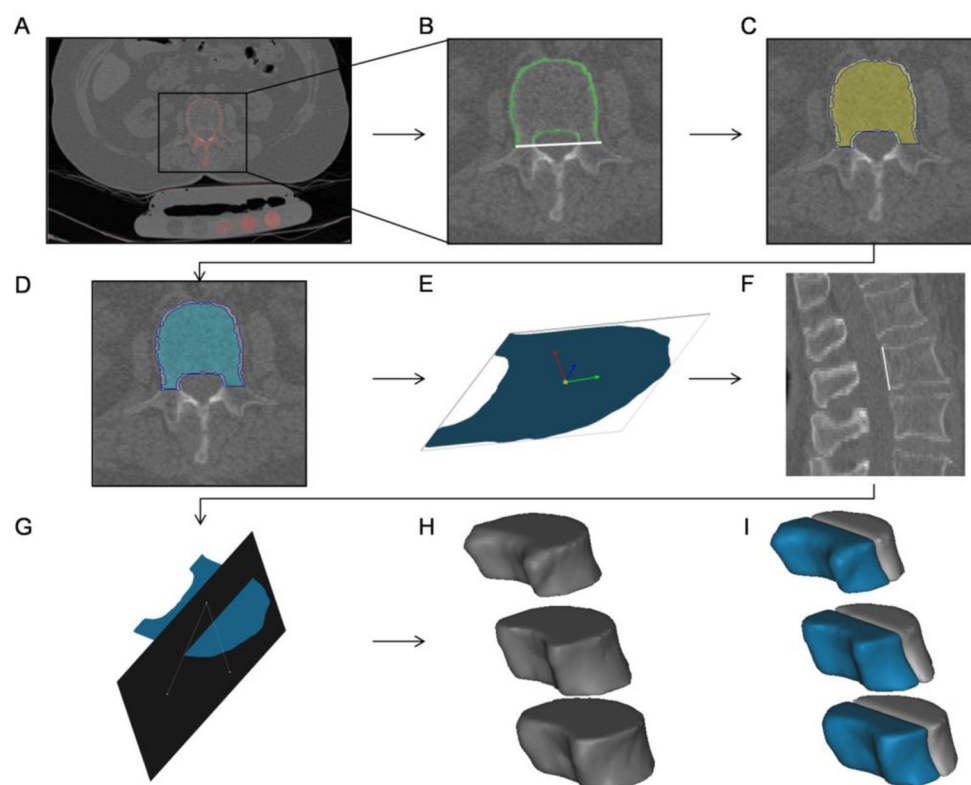


**Figure 1.**

QCT-DICOM images including patient scan with calibration phantom were uploaded and analyzed with Mimics. A) Cortical bone was defined using a Hounsfield unit-window threshold. B) Enclosed vertebral body with white line defining posterior body boundary. C) Polylines (blue) enclosing the segmented cortical and trabecular bone regions. D) Trabecular bone excluding cortical regions was segmented in all three vertebrae. E) 3D object of coronal slice showing the inertia axis. F) Line passing through the posterior boundaries of the vertebra. G) Plane dividing the trabecular vertebral body into anterior and posterior regions. The plane was defined based on the posterior line (F) and the origin of inertia axis (E). (H-I) Whole body, anterior and posterior trabecular bone regions.

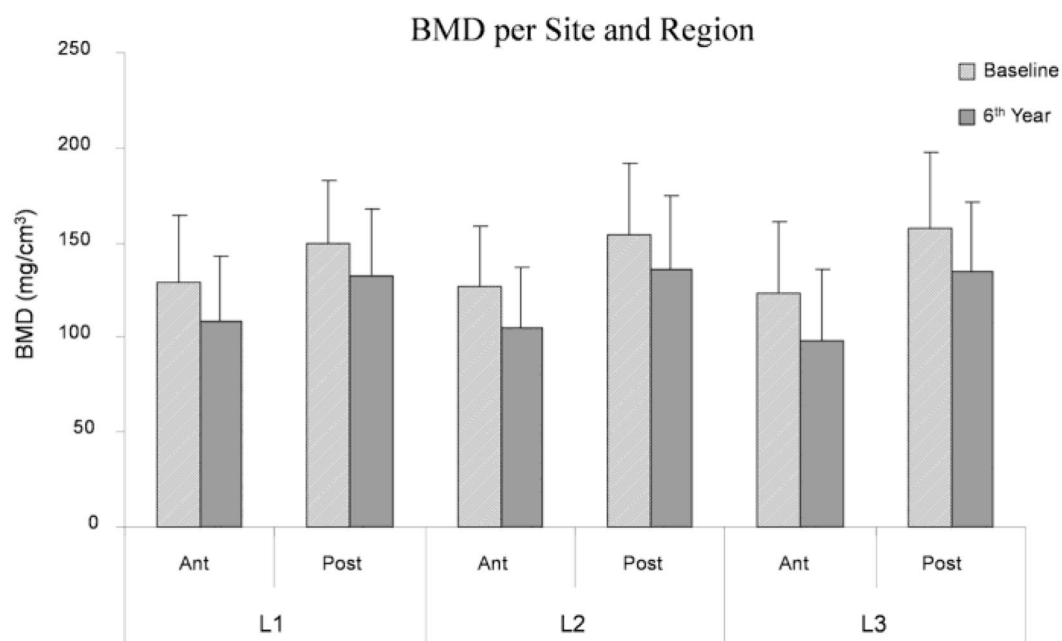


**Figure 2.** Descriptive graph presenting the acquired data based on site (L1, L2 and L3) and region (anterior and posterior) at baseline and 6<sup>th</sup> year for the 33 subjects.

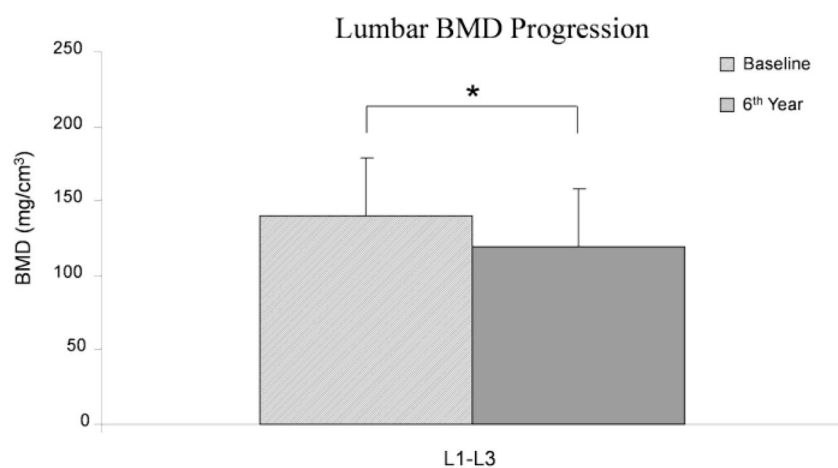


**Figure 3.** Lumbar BMD progression. L1, L2 and L3 whole body BMD measurements were combined to obtain the change over time for the sites. There was a significant decrease from baseline to 6<sup>th</sup> year values (\*:  $P < 0.0001$ ).

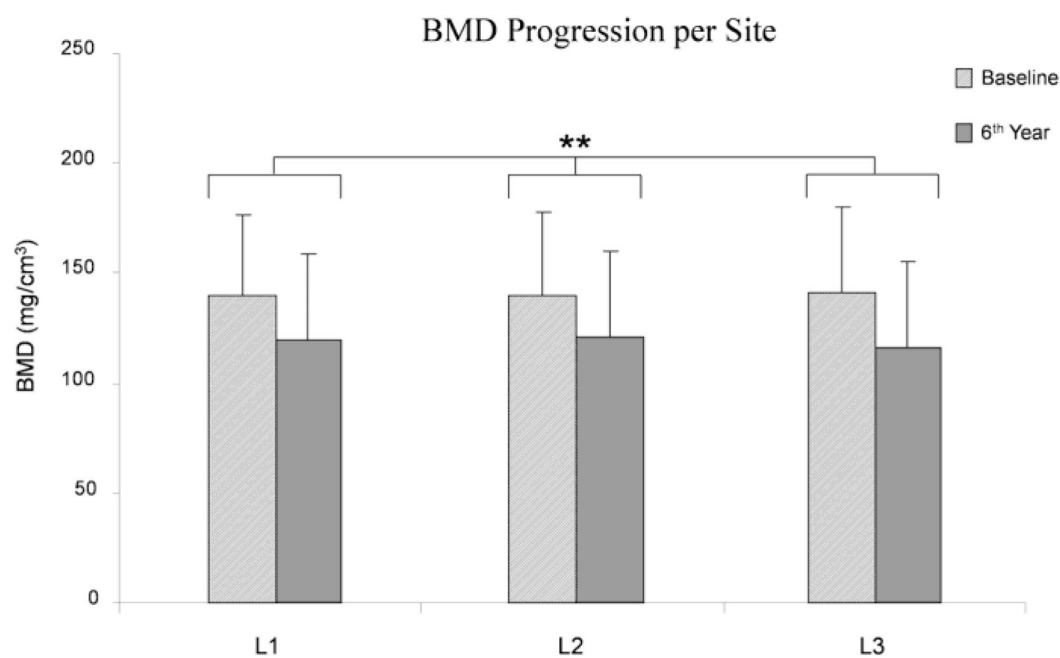


**Figure 4.** Comparison between sites over time showed to be significantly different (\*\*: $P=0.0136$ ). BMD decreased ~14% in L1, ~14% in L2 and 17% in L3.

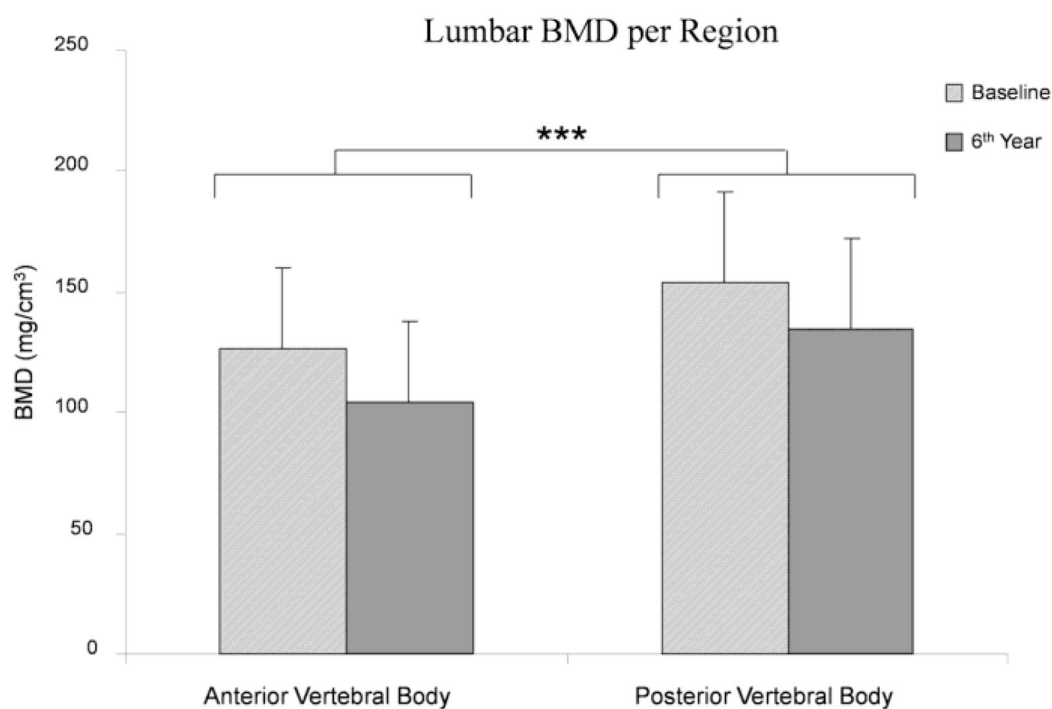


**Figure 5.** Lumbar BMD change per region. The anterior vertebral body change over time showed to be significantly greater than the posterior vertebral body decrease (\*\*\*:  $P=0.0177$ ).

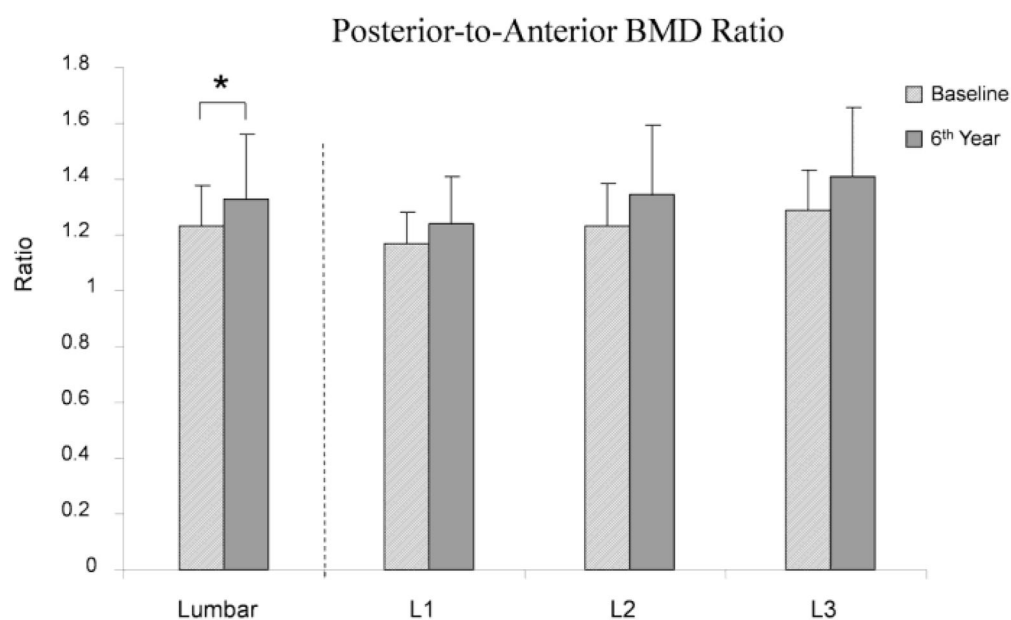


**Figure 6.** Lumbar (L1–L3) posterior-to-anterior BMD ratio was significantly greater in the 6<sup>th</sup> year compared to baseline values (\*:  $P < 0.0001$ ).

\$watermark-text

\$watermark-text

\$watermark-text

Age and BMI at baseline and 6<sup>th</sup> year are presented as mean and st. dev. Median, minimum and maximum are also presented.

Table 1

Subjects	Gender	#	Time	Label	Mean	St.Dev.	Median	Minimum	Maximum
Control	Male	21	Baseline	Age (years)	62.28	11.03	62.27	43.59	85.28
				BMI (kg/m <sup>2</sup> )	29.10	4.95	27.49	22.17	40.95
		6 <sup>th</sup> Year		Age (years)	68.24	10.95	68.42	49.48	91.38
				BMI (kg/m <sup>2</sup> )	29.93	5.61	28.57	21.14	44.54
Grade 2-3 Non-Lumbar	Male	12	Baseline	Age (years)	64.31	12.74	61.97	45.40	82.64
				BMI (kg/m <sup>2</sup> )	28.37	3.76	27.30	23.78	35.48
		6 <sup>th</sup> Year		Age (years)	70.36	12.71	67.91	51.52	88.71
				BMI (kg/m <sup>2</sup> )	28.07	3.95	27.01	23.17	35.89